

## Evaluation of site effects by means of 3D numerical modeling of the Palatine Hill, Roman Forum, and Coliseum archaeological area

R. Razzano, M. Moscatelli, M. Mancini & F. Stigliano

*Italian National Research Council – Institute of Environmental Geology and Geoengineering*

A. Pagliaroli

*University of Chieti-Pescara*

G. Lanzo

*University La Sapienza of Rome*

**ABSTRACT:** In this study we perform 3D nonlinear analyses of seismic site response of the Central Archaeological Area of Rome, which includes the Palatine Hill, Roman Forum, Circus Maximus, and Coliseum. The geological bedrock of the study area is constituted by a Pliocene marine sandy-clayey unit (Monte Vaticano Formation, MVA). At top of this unit a continental Quaternary succession is superimposed. Previous studies available for this area (Pagliaroli et al. 2014a; Mancini et al. 2014; Moscatelli et al. 2014) enabled to define a detailed three-dimensional reconstruction of the subsoil conditions, characterized by complex surficial and buried morphology, lateral heterogeneities and dynamic properties of involved material, natural as well as anthropogenic. The area of Rome is affected by earthquakes from different seismogenic districts: i) the central Apennine mountain chain ( $D = 90\text{--}130\text{km}$  and  $M = 6.7\text{--}7.0$ ); ii) the Colli Albani volcanic district ( $D = 20\text{km}$  and  $M=5.5$ ); iii) Rome area itself, which is characterized by rare, shallow, low-magnitude events ( $M < 5$ ). Both natural and artificial signals have been considered to define the input motion for the numerical modeling of the site response of the whole archaeological area. This was accomplished by means of the finite differences code FLAC3D. To evaluate the seismic hazard and, consequently, to assess possible priorities for seismic retrofitting of the monuments, contour maps of Housner intensity amplification ratio FH (defined as the ratio between Housner intensity at the top of the model and the corresponding input at the bedrock outcrop), are carried out. To cover the entire range of natural periods pertaining to the monuments in the examined area, FH was evaluated over three ranges of period: 0.1–0.5s, 0.5–1.0s, and 1.0–2.0s. Numerical results shown that: 1) within the range of periods 0.1–0.5s, high values of FH = 2.2–2.6 occur both in correspondence of narrow valleys filled with soft alluvial deposits and at top of Palatine Hill; 2) within the range of periods 0.5–1.0s, high values of FH occur in correspondence of the deepest valleys; 3) within the range of periods 1.0–2.0s, low values of FH occur except in correspondence of the deepest valleys. Results show a good agreement with the previous 2D numerical modeling and with the microzonation maps (Pagliaroli et al 2014a, b), even if interesting differences show up highlighting the usefulness of 3D modeling in such complex settings. Such results are significantly relevant for the monumental and archaeological heritage of this area, as it is highly vulnerable due to its old age and state of conservation.

### 1 INTRODUCTION

The present study reports the results of 3D numerical site response analyses for the microzonation of the archaeological areas of Palatine hill, Circus Maximus, Roman Forum and Coliseum in the historical center of Rome. The subsoil model was defined based on in situ geophysical tests and

laboratory tests to address the non-linear soil behavior. The numerical simulations are based on a subsoil model which integrates a large amount of information available from the Superintendence for the Archaeological Heritage of Rome as well as new data collected during a multidisciplinary survey conducted in 2010. Previous studies (Pagliaroli et al 2014a, b) has shown that ground motion is mainly controlled by 1D resonance phenomena and 2D effects. In order to investigate phenomena responsible for ground motion modification, the 3D numerical results are processed in terms of Housner amplification ratio (FH), defined as the ratio between Housner intensity (HI) at top of model and the corresponding input outcrop. In order to cover the entire range of natural periods of structure pertaining in the study area, three period range were considered: 0.1–0.5; 0.5–1.0; and 1.0–2.0s, and shown as contour maps.

## 2 INTRODUCTION TO THE SEISMICITY OF ROME AND SELECTION OF INPUT MOTION

The area of Rome is characterized by a low seismicity. Historical source shown that in over two thousand years of well-documented history, only eight earthquakes exceeded the damage threshold and only on three occasions in the last 1000 years the damage was serious. A comprehensive review of the historical sources that describe the earthquakes felt in Rome was performed by Molin et al. (1995) and updated by Galli and Molin (2013).

Three different seismogenic districts were considered to evaluate representative input motion for the study area: (1) the central Apennine Mountain chain, characterized by high magnitude  $M$  up to 6.7–7.0 and located about 90–130 km east of Rome; (2) the Colli Albani volcanic area with  $M=5.5$  located 20 km to the south of the city; and (3) the Rome area itself characterized by rare, shallow, low-magnitude events ( $M < 5$ ). Sabetta (2013) used both deterministic and probabilistic approach to evaluate the representative input motion for microzonation purpose (Figure 1). For probabilistic approach the UHS (Uniform Hazard Spectrum) taken from INGV was considered, having a return period of 475 years, the UHS INGV was then used to simulate spectrum-compatible time-history acceleration. Two earthquake scenarios were selected to considered the Fucino-basin, in the Apennines, and Colli Albani seismogenic districts by using both artificial and natural accelerograms. The Sabetta & Pugliese (1996) ground motion prediction was used to calculate the response spectra of these earthquake scenarios. Artificial accelerograms were then simulated compatible with the corresponding response spectra. Moreover, natural accelerograms were selected from global databases that correspond to the magnitude, distance, and soil conditions extracted for the scenario

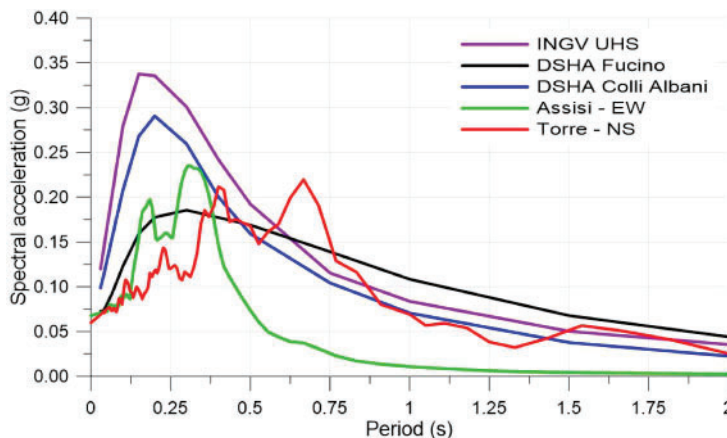


Figure 1. Reference spectra selected for the microzonation of study area.

earthquakes, including: 1) that measured at Torre del Greco during the Irpinia earthquake of 1980 for the Colli Albani scenario; and 2) that registered at Assisi during the Umbria–Marche earthquake of 1997 for the Fucino scenario.

### 3 GEOLOGICAL SETTING AND INTEGRATE SUBSOIL MODEL

#### 3.1 Morphological and geological setting

The geological bedrock of the Palatine Hill and surrounding areas consists of a Pliocene clayey-sandy unit of marine origin, the Monte Vaticano Formation (MVA in Figure 2; Mancini et al. 2014), whose total thickness is about 900 m.

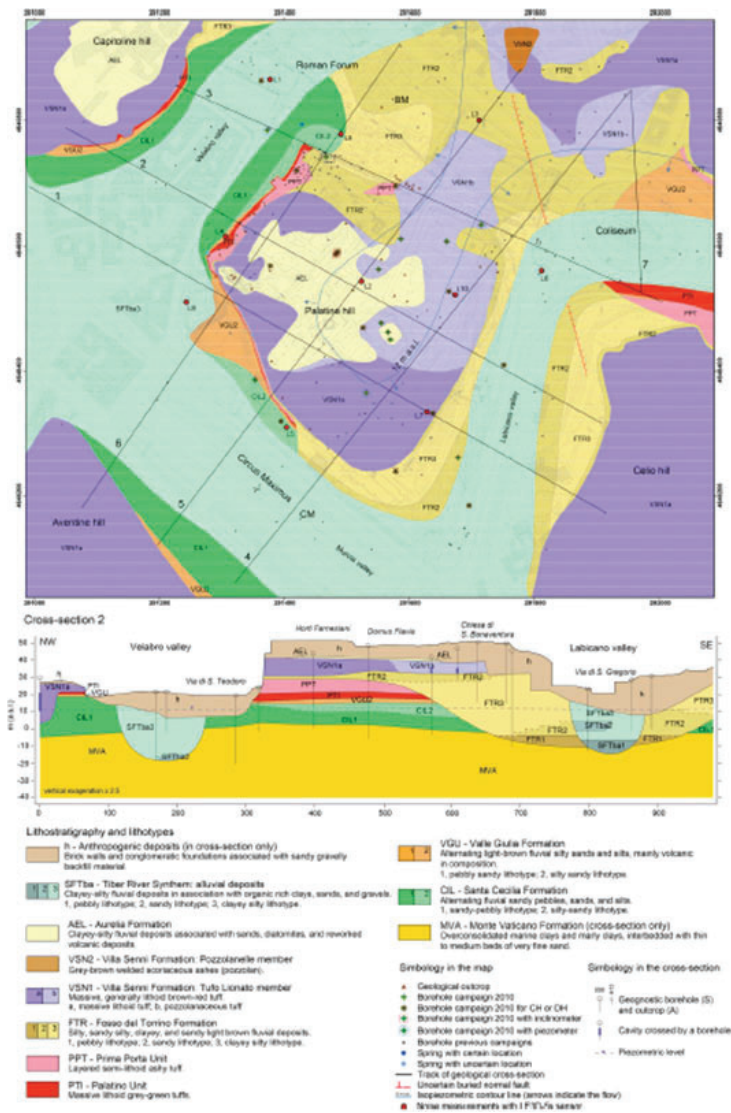


Figure 2. Geological map (above) and cross-section 2 (below) of the Palatine hill and surrounding areas (Mancini et al. 2014; Pagliaroli et al. 2014). The geological map shows the areal distribution of natural lithostratigraphic units below the anthropogenic cover deposits (10–20 m thick), not represented on map.

The top of this unit is cut by an unconformity, over which is deposited a Quaternary complex formed by the following middle Pleistocene fluvial-palustrine and distal volcanic deposits (Figure 2), listed from oldest to youngest: (1) Santa Cecilia Formation (CIL); (2) Valle Giulia Formation (VGU); (3) Palatine Unit (PTI); (4) Prima Porta Unit (PPT); (5) Fosso del Torrino Formation (FTR); (6) Villa Senni Formation (VSN), with the Tufo Lionato (VSN1) and Pozzolanelle (VSN2) members; (7) Aurelia Formation (AEL).

These formations have a sub-horizontal multilayered distribution, except for the Fosso del Torrino Formation (FTR) that fills a fluvial paleo-valley that deeply cuts into older Quaternary units in the eastern part of the Palatine Hill (see Figure 2, cross-section 2). All these units were locally carved by minor tributaries of the Tiber River during the Late Pleistocene sea-level fall, giving rise to deep (up to 70–80m) and narrow alluvial valleys (i.e. the Velabro, Labicano, and Murcia valleys; Figure 2). These valleys were mainly filled with organic-rich clayey sediments in response to the Holocene sea level rise (SFTba3 in Figure 2). The study area is almost entirely covered by anthropogenic deposits that can locally reach 20m in thickness. All the formations recognized in the study area have been interpreted in terms of lithofacies, on the basis of their sedimentological and lithological features. The lithofacies have then been grouped into geotechnical lithotypes (see legend of Figure 2), each characterized by similar index properties (e.g., grain size distribution, void ratio, unit weight, plasticity index), determined from laboratory geotechnical tests.

### 3.2 Geotechnical characterization

A large amount of subsoil information, including geophysical and geotechnical data, is available mainly from archaeological studies, from the design of adjacent subway lines and level 3 Seismic Microzonation (SM3) study (Moscatelli et al. 2014a) carried out in the framework of a large research project sponsored by the Italian Department of Civil Protection aimed at the geological and seismic hazard evaluation in the Central Archaeological Area of Rome.

In particular, the multidisciplinary survey carried out in 2010–2011 for SM3 study included continuous-coring boreholes, in situ and laboratory (dynamic and cyclic) geotechnical tests as well as different geophysical tests (MASW, cross- and down-hole tests, electrical resistivity tomography and ground penetrating radar surveys). The reconstruction of the buried morphology below the anthropic layer as well as its composition is reported in Moscatelli et al. (2014b). A subsoil model aimed at site response analyses for the seismic microzonation of the area was then built by characterizing both the man-made and natural geological materials (Pagliaroli et al. 2014a).

The subsoil numerical model for seismic response analyses requires the characterization of each unit in terms of unit weight ( $\gamma$ ), shear wave velocity ( $V_S$ ), compression wave velocity ( $V_P$ ) or, similarly, Poisson ratio ( $\nu$ ); the variation of normalized shear modulus ( $G/G_0$ ) and damping ratio ( $D$ ) with shear strain amplitude ( $\gamma_c$ ) is also required. The S-wave velocities ( $V_S$ ) were determined from a total of 17 Cross-Hole tests, 11 Down-Hole tests, 3 Seismic Dilatometer tests, and 20 MASW tests. In general, the results show that the geophysical parameters of each lithotype are spatially uniform over the entire study area and no significant gradient with depth has been observed (Pagliaroli et al., 2014a). Each lithotype was therefore characterized by averaging  $V_S$  and  $V_P$  across the different depth ranges explored. An exception is constituted by the anthropogenic layer ( $h$ ), generally formed by soil of variable grain size and masonry with extremely variable weathering, showing wide spatial heterogeneity and therefore a pronounced variability of mechanical properties. Pagliaroli et al. (2014c) carried out 2D simulations by considering in the model twenty different  $V_S$  distributions in the layer  $h$  obtained from geostatistical conditional simulations considering the spatial variability of this parameter and honoring its available measurements. Profiles of stochastic amplification factors were therefore derived at the surface. In this work, to overcome a 3D complex geostatistical simulation, an average constant value of  $V_S$  computed from all measurements was considered in the anthropogenic layer.

The normalized shear modulus  $G(\gamma_c)/G_0$  and the damping ratio  $D(\gamma_c)$  variation with shear strain amplitude were measured from a total of 20 resonant columns, 2 cyclic torsional shear tests available and 12 cyclic simple shear tests (Pagliaroli et al. 2014a). For gravelly soils (e.g., CIL1), for which

undisturbed sampling was not possible, reference was made to literature data obtained on materials having a similar granulometric distribution (Pagliaroli et al. 2014a). The same curves were used for the anthropogenic layer (h), given the prevalence of coarse material. Where multiple laboratory determinations for the same lithotype were available, the average range of the curves was used. Note that the Aurelia Fm. (AEL), because of its small thickness, was not considered in the numerical model and its thickness was assigned to the anthropogenic unit.

### 3.3 *FLAC3D numerical model*

Numerical analyses have been carried out by using the finite differences code FLAC3D (ITASCA consulting group, 2019). This code operates in time domain and implement a fully non-linear procedure to describe the soils behavior. Hysteretic-Damping model (implemented in FLAC3D) and calibrated on  $G(\gamma_c)/G_0$  and  $D(\gamma_c)$  curves was used to take into account the soil behavior with the shear strain, associate with Masing rules to describe the un-loading re-loading conditions. Rayleigh formulation was used, to account for damping at small strains, by using two control frequencies ( $f_1 = 1\text{Hz}$  and  $f_2 = 10\text{Hz}$ ). Free-field conditions (local boundaries) was applied at vertical sides of models and a quiet-base (elastic base) at bottom one to take into account the radiation damping behavior.

Nine units were considered, for numerical simulations, roughly grouping the lithotypes characterized by minor thickness and similar VS (Pagliaroli et al. 2014). SFTba3 lithotype properties were adopted for soft-filled valley unit (SFTba unit), because SFTba1 and SFTba2 are characterized by negligible thickness. Instead, for FTR paleo-valley the average value between FTR1, FTR2 and FTR3 were adopted for numerical results. The representative section with the units adopted for numerical simulations is shown in Figure 4 (cross-section #2) and in Table 1 the corresponding linear properties adopted. In Figure 3 are shown the normalized shear modulus  $G(\gamma_c)/G_0$  and damping ratio  $D(\gamma_c)$  variation with shear strain amplitude used for each lithotype, available for several laboratory test available from previous surveys in the area. It should be noted that the measured damping ratio  $D(\gamma_c)$  was not used because of Masing criteria.

The seismic bedrock is located at 500m below the ground surface, and to reduce time consuming time histories it was propagated in 1D conditions (Pagliaroli et al. 2014) and applied at the base of 3D model as outcrop motion. The identification of bedrock and the Vs profile in the MVA layer was carried out by Pagliaroli et al 2014, by integrating deep borehole and extensive noise measurements survey and 1D parametric site response analysis.

In choosing the maximum element size (hmax), the standard rule suggested by Kuhlemeyer & Lysmer (1973) was adopted to achieve a satisfactory level of solution accuracy, these authors assumed  $h_{max} = \lambda/(6 \div 8)$ , where  $\lambda = VS/(f_{max})$  is the half wavelength, VS = material shear wave velocity value selected accordingly to the shear strain level,  $f_{max}$  = maximum frequency to be

Table 1. Integrated subsoil model for site response analyses.

Lithotype (-)	Symbol (-)	$\gamma$ (kN/m <sup>3</sup> )	VS (m/s)	$\nu$ (-)
Brick walls and conglomeratic	RPI_AEL	18.0	350	0.42
Clayey-silty fluvial deposit	SFTba	18.5	270	0.49
Massive lithoid tuff	VSN1a	16.0	600	0.4
Pozzolanaceous tuff	VSN1b	19.7	340	0.48
Tuff	PTI_PPT	16.0	650	0.39
Silty, sandy silty	FTR	20.1	510	0.465
Silty sand	CIL1_2	20.1	480	0.435
Sandy pebbly	CIL1	20.5	620	0.39
OC marine clay	MVA	20.5	550	0.48



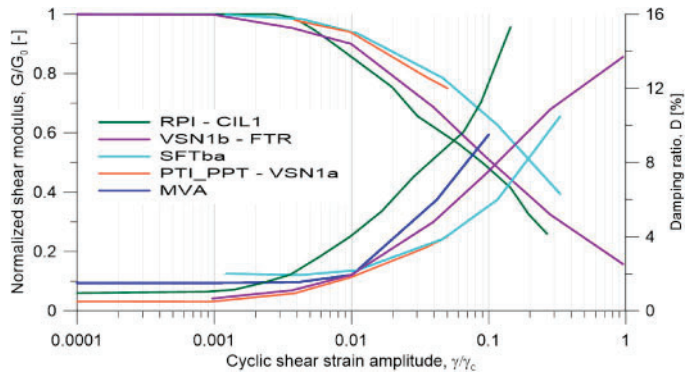


Figure 3. Non-linear behavior of soils and soft rocks:  $G(\gamma_c)/G_0$  and  $D(\gamma_c)$  curves selected for each lithotype and assumed in the integrated subsoil model.

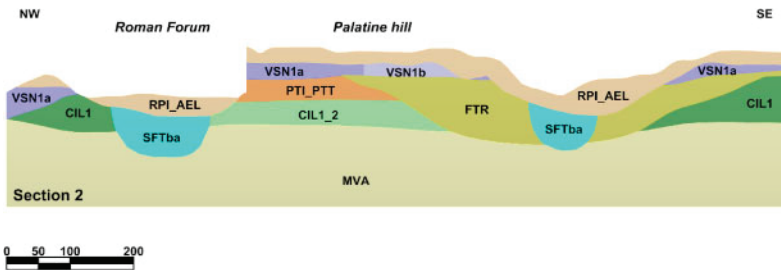


Figure 4. Cross section 2 that illustrate the units adopted for numerical results.

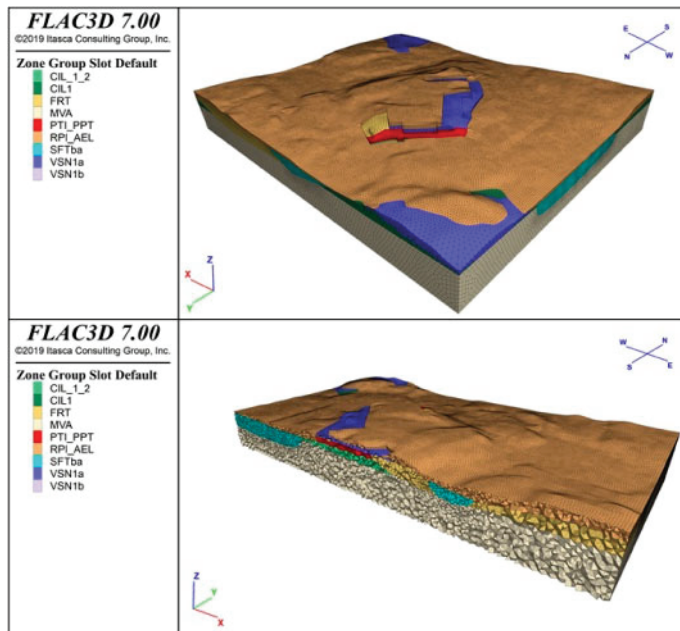


Figure 5. FLAC3D numerical grid used for numerical results.

transmitted (assumed equal to 10Hz). The 3D finite differences grid consists of about 1 million of tetrahedral shape elements (4).

#### 4 NUMERICAL ANALISES FOR MICROZONATION PURPOSES

To evaluate seismic amplifications in the study area, for microzonation purposes, three-dimensional numerical results were processed in terms of Housner Intensity (HI) over the period ranges T1–T2. In order to cover the entire range of natural vibration of the structure pertaining in the study area three different period ranges were considered: 1) 0.1–0.5s; 2) 0.5–1.0s; and 3) 1.0–2.0s.

To combine the Housner Intensity for EW and NS components Equation 1 was used:

$$HI_{T1-T2} = \sqrt{HI_{T1-T2}EW^2 + HI_{T1-T2}NS^2} \quad (1)$$

where  $HI_{T1-T2}EW$  and  $HI_{T1-T2}NS$  representing the Housner intensity for EW and NS components, respectively. The corresponding amplification factor  $FH_{T1-T2}$ , defined as the ratio between HI at ground surface and the corresponding input outcrop, were then calculated and showed as amplification maps (microzonation maps).

The first mode period of few-story masonry buildings, small-to-medium size monuments (like free-standing columns, walls, arches) generally falls in the 0.1–0.5s range (see Marzi et al. 1990 among others). Large monuments pertaining in the study area, such as Coliseum, are characterized by first mode period comprised in 0.5–1.0 s range (Pau & Vestroni 2008, 2013). It should be noted that the first two ranges T1 = 0.1s and T2 = 1.0s ( $f = 1-10$ Hz) containing the natural frequencies vibration of the most of structures pertaining in the study area. The results are discussed below to illustrate major findings of the morphological, geological and mechanical characteristics of the whole area.

In Figure 6 is shown the contour map of  $FH_{0.1-0.5}$  amplification factor, obtained by assuming T1-T2 = 0.1–0.5s (frequencies range 2–10Hz), that exhibit strong variations in the study area. The highest values of  $FH_{0.1-0.5}$  (up to 2.2–2.6) occur in correspondence of Velabro valley, located in North-West part of model, where the incised soft-filled valley (SFTba unit with VS = 270m/s) become narrow (see cross-section 3 in Figure 7). This is related to the resonance frequencies of valley, in this area, which is around 2.5–3.0Hz computed according to the formula proposed by Bard & Bouchon (1985).

$FH_{0.1-0.5}$  fluctuate between 1.6, passing from the confluence of Murcia and Labicano valleys (located in south part of model) filled by soft-filled valley (SFTba) like Velabro valley, to 2.4 in correspondence of Coliseum area. Instead, moderate values in Murcia valley up to 1.4–1.6 (Circus maximus area), because the soft SFTba unit become more deepest (see cross-section 6 in 5).

At top of Palatine hill  $FH_{0.1-0.5}$  exhibit strong fluctuations, probably due at the complex surficial and buried morphologies, e.g. the multilayered deposit and FTR paleo-valley. The greater amplifications are located in Horti Farnesiani probably for the 1D resonance of the soft anthropogenic layer overlying the stiffer VSN1a lithoid tuff and near Vigna Barberini, at the edge of the FTR paleo-valley, with VS = 510m/s (Figure 6).

Instead,  $FH_{0.1-0.5}$  decrease up to 1.0–1.2 where FTR deepens (Via dei Fori Imperiali). The lower amplifications at hill toe ( $FH_{0.1-0.5} = 1.0-1.2$ ) can be ascribed to deamplification for topographic effects, as observed by Pagliaroli et al. 2014b.

Amplification factors  $FH_{0.5-1.0}$  and  $FH_{1.0-2.0}$  (that corresponding at frequencies range 1–2 Hz and 0.5–1 Hz, respectively) exhibit similar trends but different values, the corresponding amplification maps are shown in Figures 8 and 9, respectively. The effects of the incised soft-filled valley (SFTba unit) is evident. Indeed,  $FH_{0.5-1.0}$  up to 2.2–2.4 and  $FH_{1.0-2.0}$  up to 1.8–2.0 occur at the confluence between the Murcia and the Tiber Valleys (located outside the figures to the west), that represent the zones where the soft-filled valley are deeper (about 40m), in the examined area (see cross-sections 1 and 6 in 5).

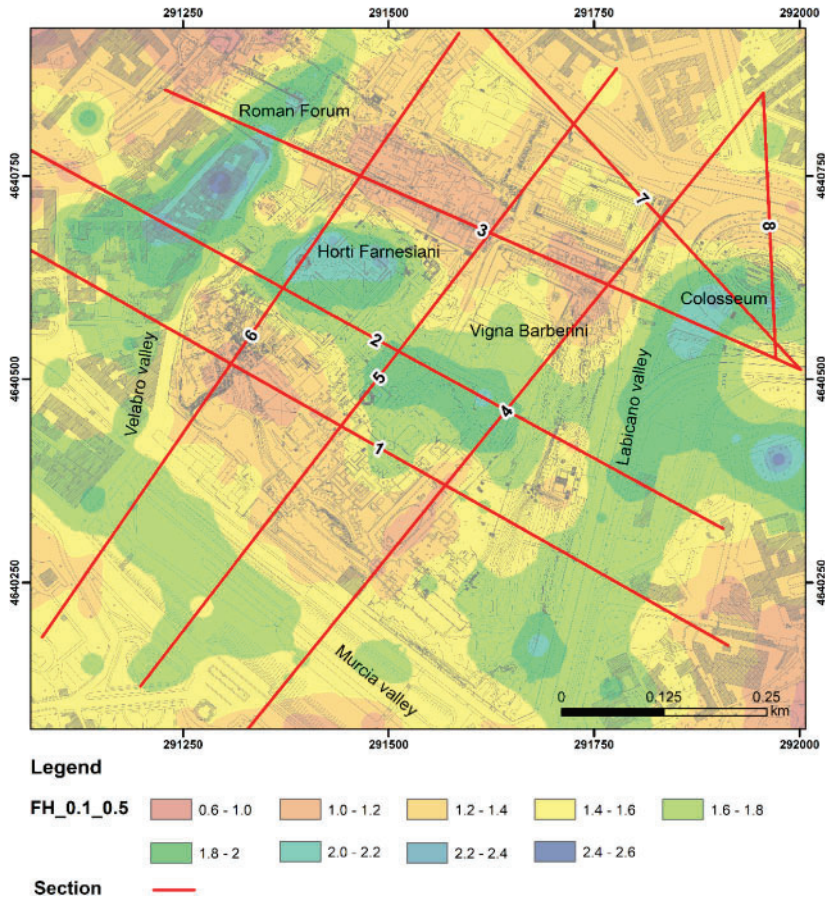


Figure 6. Contours map of amplification factor  $FH_{0.1-0.5}$ , red lines representing the cross-sections.

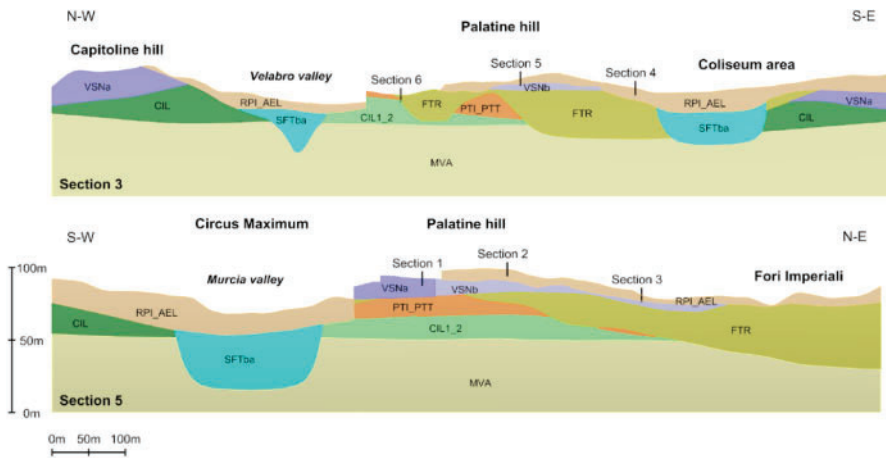


Figure 7. Cross-section 3 (above) and 5 (below), vertical exaggeration 2.



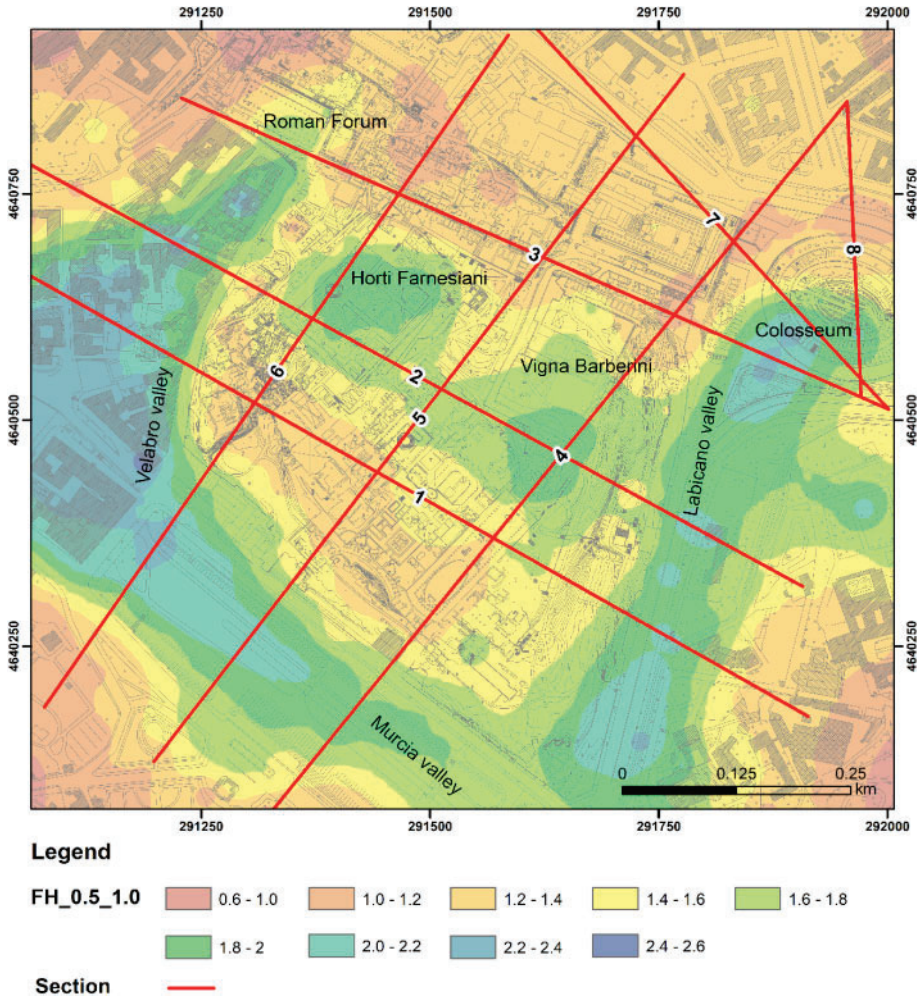
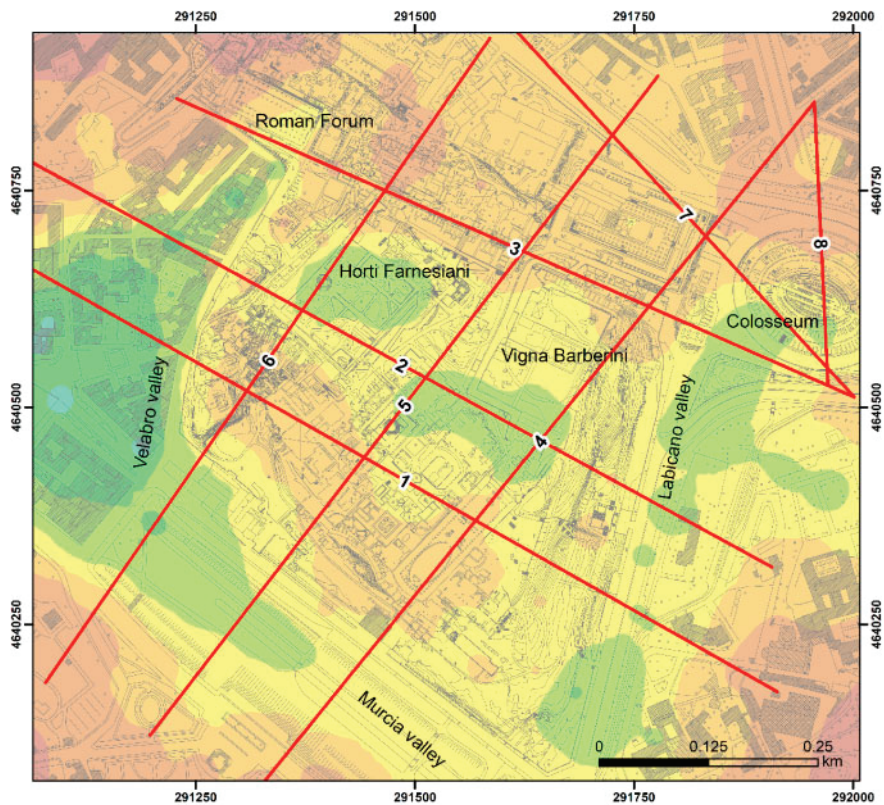


Figure 8. Contours map of amplification factor  $FH_{0.5-1.0}$  (obtained by assuming  $T_1=0.5s$  and  $T_2=1.0s$ ), red lines representing the cross-sections.

In the SFTba unit, bordering the Palatine hill,  $FH_{0.5-1.0}$  exhibits great amplifications up to 1.8–2.0 in Murcia and Labicano valleys, and up to 2.0–2.2 in the Coliseum area. Instead,  $FH_{1.0-2.0}$  amplifications decrease up to 1.4–1.6.

At top of Palatine hill both  $FH_{0.5-1.0}$  and  $FH_{1.0-2.0}$  amplification factors exhibit moderate values, except at Horti Farnesiani and Vigna Barberini ( $FH_{0.5-1.0}$  around 1.8–2 and  $FH_{1.0-2.0}$  about 1.6–1.8).

Generally, for the three period ranges considered in this study, the soft-filled valleys bordering the Palatine hill (SFTba unit) exhibit the highest values of  $FH_{T_1-T_2}$  by varying the period considered, because the valley is characterized by variable thickness and width (see Figures 7 and 5). The three amplification factors ( $FH_{0.1-0.5}$ ,  $FH_{0.5-1.0}$ ,  $FH_{1.0-2.0}$ ) show quite different trends from both a qualitative and quantitative point of view, highlighting the “filter effect” that the soft rock and soil deposits exert on seismic motion (as a function of their mechanical and morphological features).



**Legend**



**Section**



Figure 9. Contours map of amplification factor FH1.0-2.0 (obtained by assuming  $T_1=1.0$ s and  $T_2=2.0$ s), red lines representing the cross-sections.

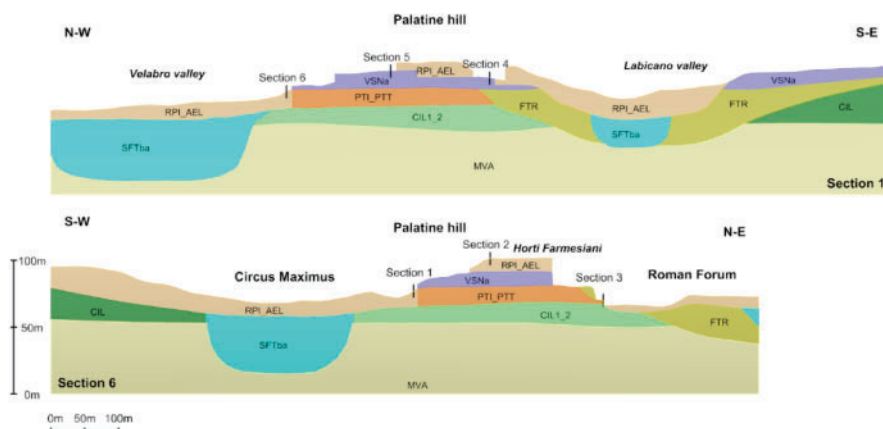


Figure 10. Cross-sections 1 (above) and 6 (below), vertical exaggeration 2.

## 5 CONCLUSIONS

The Rome area is characterized by low local seismicity, however the Apennine faults, characterized by high magnitude and distances, can produce strong effects in highly vulnerable structures due at phenomena of local amplification of the seismic motion. These latter are due to the complex local conditions: stratigraphic and morphological-topographic. This study presents local seismic response of the Central Archaeological Area of Rome based on a three-dimensional numerical model. Numerical results are carried out by using the finite differences code FLAC3D. A considerable number of investigations on site and in the laboratory are used to define the subsoil model. Numerical results are processed in terms of Housner Intensity over three period ranges T1-T2. In order to cover the entire range of natural periods of structures pertaining in the study area three period ranges were considered: 1) 0.1–0.5; 2) 0.5–1.0; 1.0–2.0s. The corresponding amplification factor FHT1-T2, defined as the ratio between HI at ground surface and the corresponding input outcrop, were then calculated and showed as contours maps (amplification maps).

At period range T1-T2 = 0.1–0.5s (frequencies range 2–10Hz) amplification factor FH<sub>0.1-0.5</sub> exhibit strong fluctuation in the study area, values up to 2.4 are located in the zones where the soft-filled valley (SFTba unit), bordering the Palatine hill, become narrow (Roman forum) and at top of Palatine hill (Horti Farnesiani and Vigna Barberini) probably due to the complex stratigraphic and topographic setting.

Instead, period ranges T1-T2 = 0.5–1.0s and 1.0–2.0s (that corresponding at frequencies range 0.5–2.0Hz) the amplification factor FH<sub>0.5-1.0</sub> and FH<sub>1.0-2.0</sub> exhibit similar trend. The greater amplifications, up to 2.4–2.6, are located in the zone where the soft-filled valley (SFTba unit) deepens (Labicano and Velabro valley).

Pagliaroli et al. (2014a and b) carried out the same amplification maps (with the same period ranges and time histories) numerical results were obtained by interpolating the 2D equivalent-linear simulations, performed by using the finite difference code QUAD4M, on seven cross-sections.

2D maps exhibit minor amplification and fluctuations as compared as 3D ones: i) FH<sub>0.1-0.5</sub> and FH<sub>0.5-1.0</sub> maps shown amplification up to 1.8 for 2D conditions and 2.6 for 3D ones; ii) FH<sub>1.0-2.0</sub> maps are essentially flat in 2D conditions with maximum amplifications up to 1.3 in correspondence of Vigna Barberini, instead 3D ones exhibit amplifications about twice located in the soft-filled valley, Vigna Barberini and Horti Farnesiani. The comparisons between 3D and 2D highlighted the role of 3D effects on seismic response, of study area, due at complex buried and surficial morphologies.

Even if the amplification factor exceeds 2.6 only in limited areas (soft-filled valley unit), the importance of these changes in ground motion can be significant for the highly vulnerable monumental and archaeological heritage within the study area.

## REFERENCES

- Bard P.Y. & Bouchon M. 1985. The two-dimensional resonance of sediment-filled valleys. *Bull Seismol Soc Am* 75:519–541
- Itasca Consulting Group, Inc. (2019) *FLAC3D — Fast Lagrangian Analysis of Continua in Three-Dimensions*, Ver. 7.0. Minneapolis: Itasca.
- Kuhlemeyer, R. L. & Lysmer, J. 1973. Finite Element Method Accuracy for Wave Propagation Problems. *Journal of the Soil Dynamics Division*, 99, 421–427.
- Mancini M. et al. 2014. A physical stratigraphy model for seismic microzonation of the Central Archaeological Area of Rome (Italy). *Bulletin of Earthquake Engineering*, 12, 1339–1363.
- Marzi C. et al. 1990. Seismic preservation of historical monuments in Rome: preliminary results from ambient vibration tests. In: Marinos, Koukis (eds) *Engineering geology of ancient works, monuments and historical sites*, pp 2133–2134
- Moscatelli M. et al 2014a. Seismic microzonation of Palatine hill, Roman Forum and Coliseum Archeological Area. *Bulletin of Earthquake Engineering* 12, 1269–1275.

- Moscatelli M. et al. 2014b. Integrated geological and geophysical investigations to characterized the anthropic layer of Palatine hill and Roman Forum. *Bulletin of Earthquake Engineering* 12, 1319–1338.
- Pagliarioli A. et al. 2014a. Dynamic characterization of soils and soft rocks of the Central Archaeological Area of Rome. *Bulletin of Earthquake Engineering*, 12, 1365–1381.
- Pagliarioli A. et al. 2014b. Numerical modelling of site effects in the Palatine hill, Roman Forum and Coliseum archaeological area. *Bulletin of Earthquake Engineering*, 12, 1383–1403.
- Pagliarioli A. et al. 2014c. Seismic microzonation of the Central Archeological Area of Rome: results and uncertainties. *Bulletin of Earthquake Engineering*, 12, 1405–1428.
- Pau A. & Vestroni F. 2008. Vibration analysis and dynamic characterization of the Colosseum. *Struct Control Health Monit* 15:1105–1121.
- Pau A & Vestroni F. 2013. Vibration assessment and structural monitoring of the Basilica of Maxentius in Rome. *Mech Syst Signal Process*.